

TOWARDS THE PREDICTION  
OF WELD METAL PROPERTIES

by

Alastair Allen Brockbank Sugden  
Robinson College  
Cambridge

A dissertation submitted for the fulfilment  
of the Degree of Doctor of Philosophy  
at the University of Cambridge

September 1988

VOLUME 1

*Mieux vaut prévoir sans certitude que de ne pas prévoir du tout.*  
It is far better to predict without certainty, than never to predict at all.  
*J. H. Poincaré, LA SCIENCE ET L'HYPOTHESE.*

to

Elizabeth Claire Sugden

## PREFACE

**T**HIS DISSERTATION is submitted for the degree of Doctor of Philosophy at the University of Cambridge. The work described was carried out at the Department of Materials Science and Metallurgy, Cambridge, between October 1985 and September 1988.

All the work presented in this dissertation is original work (except where specific reference is made to the contrary), and has not been submitted in whole or in part for a degree or diploma.

I am grateful to the Science and Engineering Research Council for financial support, to ESAB AB (Sweden) for financial support and for provision of laboratory facilities, and to Professor D. Hull for the provision of laboratory facilities at the University of Cambridge.

This dissertation contains less than 60,000 words.

*Alain Sunde*  
.....  
29/9/88

## ACKNOWLEDGEMENTS

I am grateful to many people for the help and advice they have given me throughout this work. Firstly, I am indebted to Dr. Harry Bhadeshia for the invaluable advice and unfailing encouragement he has supplied throughout this course of research, and whom I have been fortunate to have as a supervisor. His enthusiasm, also, has been a constant source of inspiration.

Secondly, I would like to thank Dr. Lars-Erik Svensson for the interest he has shown in the project, and to all the members of the Göteborg research team, in particular Mrs. Berit Gretoft, Drs. Bengt Utterberg and Leif Karlsson, for a happy, productive, and memorable stay in Sweden. Nearly all the welds used in this research were fabricated and chemical analyses performed at the laboratories of ESAB AB (Sweden) in Göteborg, and this is acknowledged here. I would also like to thank Dr. Pete Wilkins of Murex (Waltham Cross) for organizing the manufacture of special weldments. Technical assistance from Mr. Tony King at the Cavendish laboratory is also acknowledged.

I am grateful to Dr. John Knott for the helpful advice he has given me on fracture theory, and also to Mrs. Helen Druiff for her help in explaining the various aspects of the theory of tensile testing. Thanks are due to Mr. Tim Mortimer and Dr. Pat Altham of the Department of Pure Mathematics and Mathematical Statistics for explaining a variety of statistical techniques to me, and to Mike O'Donohoe for teaching me how to use the algorithm library on the mainframe. A very special thanks goes to Dr. Pat Stewart for her help and kindness in teaching me how to use  $\text{\TeX}$ .

It is a pleasure to acknowledge the whole of the Phase Transformations Group (Ashraf Ali, Serdar Atamert, Moazam Baloch, Naseem Haddad, Shahid Khan, Roger Reed, Sunil Sahay, Martin Strangwood, Manabu Takahashi, Peter Wilson, and Jer-Ren Yang), and the erstwhile Steel group (Paulo Rios and Bilgin Soylu) for their encouragement and stimulating discussions, particularly, Serdar Atamert and Jer-Ren Yang for the help they gave me concerning transmission electron microscopy. I promised Naseem Haddad that if he taught me how to use the electropolisher I would acknowledge this, too.

I would to thank Messrs. Brian Barber and Maurice Swann for their enormous help over the last three years in preparing many slides and negatives for me, and for their advice on photography. Machining of many of the weld specimens was carried out by Messrs. Graham Morgan, Pete Hull, and Mick Brand.

I am grateful to Mrs. Gillian Burrows of the Scientific Periodicals Library for the many hours of book-hunting she has spent on my behalf, to the library staff at the Welding Institute, in particular Mrs. Janet Herridge, to Mrs. Helga Olsson at the ESAB library in Sweden, and to the librarian at the Cambridge University Engineering Library.

Thanks are due, too, to Mrs. Sheila Barkham for her contribution to the typing of this manuscript.

Finally, I would like to thank my family for their constant support throughout this project.

## ABSTRACT

A large amount of work has recently been done on the prediction of the microstructure of steel weld deposits, making it possible now to estimate the as-welded microstructure as a function of thermal history and chemical composition. This work is part of a complementary project aimed at obtaining quantitative and widely applicable relationships between weld microstructures and properties.

The thesis begins with a literature review covering the major features of the development of microstructure in low-alloy steel welds, and the recent work on the modelling of this microstructure. A variety of factors influence the relation between microstructure and mechanical properties. The microstructure and properties of a weld are influenced strongly by the mode of solidification, whether this involves the formation of  $\delta$ -ferrite or austenite as the primary phase, and the solidification stage determines the extent of chemical segregation and growth processes within the weld pool. Experimental work has been carried out to determine the cooling rates at the solid-liquid interface encountered in weld pools as a function of welding conditions. The critical carbon composition for low-alloy steel welds above which solidification will occur as austenite has also been established for the manual-metal-arc process. Thermodynamic models have been employed and developed to allow the various phase transformations experienced by low-alloy steels during equilibrium solidification to be calculated for any reasonable combination of alloying elements. Calculations for the partition coefficients of solute elements during solidification are also presented. This work should provide a basis for the calculation of time-temperature-transformation diagrams for the solidification process.

Detailed models are presented to allow the quantitative prediction of weld metal yield strength, tensile strength, flow stress, strain hardening characteristics, elongation, and reduction of area for a given microstructure and composition. The model for tensile strength is further developed to allow strength to be calculated as a function of temperature. The wide scatter in toughness results often associated with weld metals is shown to be explicable in terms of the inhomogeneity of the microstructure.

Any attempt at modelling the toughness of welds requires a knowledge of the

inclusion distribution. Work on experimental welds has shown that the inclusions in a weld deposit are not uniformly distributed, but segregate to the boundaries of the first phase to solidify. The implications of this work are particularly serious for welds solidifying as austenite, since the inclusions are then located away from the centres of the grains where they cannot act as intragranular nucleants for acicular ferrite. In a separate chapter, fresh evidence that the acicular ferrite phase in welds is bainitic is presented.

In summary, the thesis presents work which has successfully modelled some of the important mechanical properties of welds, and work which has laid the foundations for further research aimed at obtaining quantitative microstructure-property relationships.

# CONTENTS

## VOLUME 1

Preface . . . . .	i
Acknowledgements . . . . .	ii
Abstract . . . . .	iv
Contents . . . . .	vi
List of Principal Abbreviations . . . . .	xi
List of Principal Symbols . . . . .	xii

## CHAPTER ONE

### Some Aspects of Welding Metallurgy

1.1 Introduction . . . . .	1
1.2 The Arc Welding Process . . . . .	1
1.3 Weld Metal Solidification . . . . .	2
1.4 The As-deposited Microstructure . . . . .	5
1.4.1 Allotriomorphic Ferrite . . . . .	5
1.4.2 Widmanstätten Ferrite . . . . .	6
1.4.3 Acicular Ferrite . . . . .	7
1.4.4 Microphases . . . . .	7
1.4.5 Idiomorphic Ferrite . . . . .	8
1.5 Inclusions . . . . .	8
1.6 A Model for the As-deposited Microstructure . . . . .	9
1.7 Reaustenitisation . . . . .	12
1.8 Summary . . . . .	12
References . . . . .	14

## CHAPTER TWO

### Changes in Solidification Mode, and the Measurement of Cooling Rates following Solidification during Arc Welding

2.1 Introduction . . . . .	17
2.2 Primary Solidification Structures . . . . .	18
2.3 Experimental Method . . . . .	20
2.4 Analysis of Experimental Results . . . . .	24

2.5 Summary . . . . .	27
References . . . . .	29

### CHAPTER THREE

#### The Non-Uniform Distribution of Inclusions in Low-Alloy Steel Weld Deposits

3.1 Introduction . . . . .	31
3.2 Experimental Method . . . . .	33
3.3 Results . . . . .	35
3.3.1 Weld 3.1: $L \rightarrow \gamma + L \rightarrow \gamma \rightarrow \alpha + Fe_3C$ . . . . .	35
3.3.2 Weld 3.2: $L \rightarrow \delta + L \rightarrow \delta + \gamma + L \rightarrow \gamma \rightarrow \alpha + Fe_3C$ . . . . .	36
3.3.3 Weld 3.3: $L \rightarrow \alpha + L \rightarrow \alpha$ . . . . .	37
3.3.4 Weld 3.4: $L \rightarrow \delta + L \rightarrow \delta + \gamma + L \rightarrow \gamma \rightarrow \alpha + Fe_3C$ . . . . .	37
3.4 Discussion . . . . .	38
3.5 Summary . . . . .	40
References . . . . .	42

### CHAPTER FOUR

#### Thermodynamic Prediction of the Liquidus, Solidus, and Ae3 temperatures and Phase Compositions for Low-Alloy Multicomponent Steels

4.1 Introduction . . . . .	44
4.2 The Solidification of Steel . . . . .	45
4.3 Method of Analysis . . . . .	48
4.4 Prediction of Ae3 temperature . . . . .	51
4.4 Prediction of Peritectic Region . . . . .	55
4.5.1 Liquidus Temperature . . . . .	55
4.5.2 Solidification as Primary Austenite . . . . .	60
4.5.3 Prediction of Solidification Ranges . . . . .	61
4.6 Calculation of Partition Coefficients . . . . .	62
4.7 Summary . . . . .	64
References . . . . .	66

### CHAPTER FIVE

#### A Model for the Strength of the As-deposited Regions of Low-Alloy Steel

##### Weld Metals

5.1 Nomenclature . . . . .	69
5.2 Introduction . . . . .	71

5.3 Method . . . . .	72
5.4 Choice of Guessed Values . . . . .	83
5.5 Results . . . . .	84
5.6 Using the Model . . . . .	85
5.7 Summary . . . . .	87
References . . . . .	89

CHAPTER SIX

Further Predictions about Weld Metal Strength

6.1 Introduction . . . . .	92
6.2 Experimental Method . . . . .	93
6.3 The Determination of Yield Stress from Hardness . . . . .	94
6.4 Method of Analysis . . . . .	97
6.5 Results . . . . .	100
6.6 Discussion . . . . .	101
6.2 Summary . . . . .	104
References . . . . .	106

VOLUME 2

Contents . . . . .	i
--------------------	---

CHAPTER SEVEN

The Prediction of Non-Uniform Elongation

7.1 Introduction . . . . .	1
7.2 The Stress-Strain Curve . . . . .	2
7.3 The Factors Controlling Ductility . . . . .	4
7.4 Experimental Method . . . . .	7
7.5 Results . . . . .	8
7.6 Discussion . . . . .	11
7.7 Summary . . . . .	16
References . . . . .	18

CHAPTER EIGHT

Weld Metal Ductility: Reduction in Area

8.1 Introduction . . . . .	20
8.2 Stress Intensification . . . . .	20
8.3 The Necking Process and Reduction in Area . . . . .	21
8.4 Models . . . . .	24
8.5 Discussion . . . . .	27
8.6 Summary . . . . .	29
References . . . . .	31

## CHAPTER NINE

### Scatter in Weld Metal Toughness Measurements

9.1 Introduction . . . . .	34
9.2 Analysis of Scatter . . . . .	36
9.3 Quantification of Heterogeneity . . . . .	38
9.4 Results . . . . .	40
9.5 Discussion . . . . .	43
9.6 The Effect of Tempering on Weld Metal Hardness . . . . .	43
9.7 Summary . . . . .	45
References . . . . .	46

## CHAPTER TEN

### The Discovery of Lower Acicular Ferrite

10.1 Introduction . . . . .	48
10.2 The Formation of Bainite . . . . .	49
10.3 Acicular Ferrite . . . . .	52
10.4 Experimental Method . . . . .	52
10.5 Results . . . . .	54
10.6 Discussion . . . . .	56
10.7 Summary . . . . .	57
References . . . . .	59

## CHAPTER ELEVEN

<u>A Programme for Future Research</u> . . . . .	61
References . . . . .	66

## APPENDICES

Appendix 1: Ae3 Program . . . . .	67
-----------------------------------	----

Appendix 2: Determination of $\Delta T$ . . . . .	77
Appendix 3: Peritectic Program . . . . .	82
Appendix 4: Strengthening Program . . . . .	97
Appendix 5: Strain-Hardening Coefficients Program . . . . .	114
Appendix 6: Heterogeneity Program . . . . .	117

## LIST OF PRINCIPAL SYMBOLS

- $\alpha$  allotriomorphic ferrite; alpha ferrite; liquid thermal diffusivity; experimentally determined Charpy constant
- $\alpha'$  martensite
- $\alpha_a$  acicular ferrite
- $\alpha_w$  Widmanstätten ferrite
- $\beta$  constant of proportionality (Barba's law); experimentally determined Charpy constant
- $\gamma$  austenite; specific interfacial free energy per unit area
- $\gamma_i$  activity coefficient of solute i (Raoultian standard state and mole fraction basis)
- $\gamma_r$  retained austenite
- $\delta$  delta-ferrite
- $\delta_s$  solute boundary layer thickness
- $\epsilon_f$  critical strain; fracture strain
- $\epsilon_u$  strain during uniform elongation
- $\nu$  number of degrees of freedom
- $\tau$  relative plate thickness
- $\Delta^\circ G_o^{\alpha \rightarrow \gamma}$  standard molar Gibbs free energy change accompanying, for example,  $\alpha - \gamma$  transformation in pure iron
- $\Delta^\circ H$  standard molar enthalpy change
- $\Delta^\circ S$  standard molar entropy change
- $\Delta T$  temperature deviation from  $T_o$  curve; temperature difference; undercooling
- $\Delta T_o$  total undercooling
- $\Delta T_{8-5}$  cooling time through the range 800-500°C
- $\epsilon$  Wagner interaction coefficient
- $\eta$  coefficient of viscosity
- $\theta$  wetting angle; cementite
- $\lambda$  distance between isotherms
- $\mu$  chemical potential
- $\rho_i$  density of an inclusion
- $\rho_s$  density of steel; solid density
- $\sigma_o$  flow stress
- $g_L$  fraction solidified

- $T_0$  curve defining the locus of all temperatures where austenite and ferrite of the same composition have the same free energy.
- $U$  welding voltage
- $V$  volume of particle
- $V_a$  volume fraction of acicular ferrite
- $V_w$  volume fraction of Widmanstätten ferrite
- $V_\alpha$  volume fraction of allotriomorphic ferrite
- $W_s$  Widmanstätten ferrite start temperature
- $X$  mole fraction
- $X_i$  molar solute concentration of component  $i$

# CHAPTER 1

## SOME ASPECTS OF WELDING METALLURGY

### 1.1 INTRODUCTION

Over the last decade, research in welding science has accelerated as a consequence of the increased importance of welding in the fabrication of engineering structures. However, although our knowledge of welding techniques has increased dramatically, the largely empirical approach that has been favoured in welding consumable development has meant that there is still a clear lack of understanding about which factors control the mechanical properties of structural steel weldments for the wide range of welding conditions and consumables which are encountered in practice. Consequently, there is a need for a more theoretical treatment of the subject. The present investigation aims at providing a more formal description of the factors that influence weld metal properties, and is part of a continuing programme whose eventual aim is to quantify the properties of low-alloy steel weld deposits in terms of weld metal chemical composition and thermal history.

As a brief introduction to this field of research, a review of the various aspects of welding metallurgy relevant to this work is now given. Individual topics are developed in the chapters that follow. In this review, following a brief description of arc welding, the essential characteristics of weld metal solidification are discussed, and related to general solidification theory. The current state of knowledge concerning the microstructural constituents that comprise the as-welded microstructure, and their evolution is critically reviewed, and a model that allows the prediction of this microstructure is described. Finally, the significance of re-austenitisation in controlling the microstructure of multirun weld deposits is emphasized. The review highlights many of the key areas in which further research is required, and serves as a good context in which to place the work that follows.

### 1.2 THE ARC WELDING PROCESS

In arc welding, two pieces of metal are joined together using an electric arc as an energy source, the arc most usually being established between a metal electrode

and the workpiece. The intense heat input causes regions of the joint to melt and fuse together. Manual-metal-arc (MMA) welding with coated stick electrodes is the most widely used of all fusion welding processes, and it is the technique with which this dissertation is primarily concerned. In MMA welding, the arc melts the edges of the component to be welded, and forms a weld pool in the workpiece. Simultaneously, the tip of the electrode melts, and metal drops are transferred via the arc to the workpiece (see Figure 1.1). Melting of the coating on the electrode causes a shielding gas to develop, and this protects the weld from oxygen and nitrogen in the air. The metal droplets which are transferred in the arc are covered with molten slag. On contact with the weldpool, the slag floats to the surface thus providing a protective cover on the top of the hot weld metal.

In the submerged-arc (SA) welding process, which is also widely used, the same principles apply, but the arc and metal are shielded by a blanket of granular fusible material on the workpiece during welding (Figure 1.2).

### 1.3 WELD METAL SOLIDIFICATION

The evolving microstructure in fusion welding is strongly influenced by the prevailing thermal conditions, and weld metal chemistry. Weld pool conditions are such that growth is nearly always cellular or, in more highly alloyed steels, cellular-dendritic. Under these conditions, the total undercooling is not only a function of the structure of the interface, but is also dependent upon the growth rate and temperature gradient in the liquid ahead of the growing interface. Thus, the total measured undercooling may be written as (Davies and Garland, 1975)

$$\Delta T = \Delta T_D + \Delta T_r + \Delta T_K \quad (1.1)$$

where  $\Delta T_D$  is the contribution due to the solute layer, that is, the undercooling required to give a sufficient composition difference to drive diffusion.

$\Delta T_r$  is the undercooling due to interface curvature,

and  $\Delta T_K$  is a kinetic contribution.

$\Delta T_K$ , for metals, is usually assumed to be negligible compared to other contri-

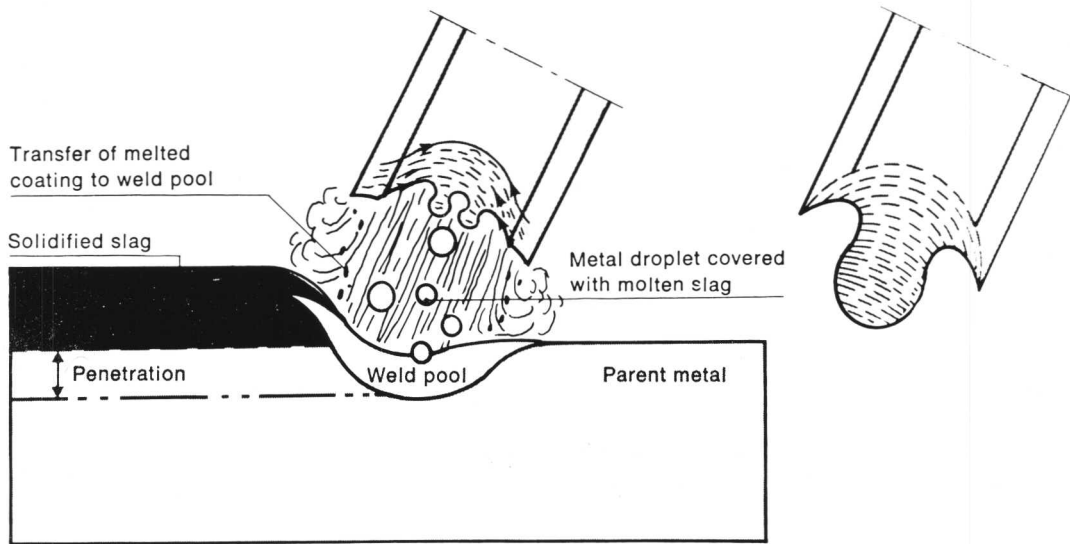


Figure 1.1: Schematic diagram of the MMA welding process. (After B. Lundqvist (1977), "Sandvik Welding Handbook", Sandvik AB, Sandvikken, Sweden, 28).

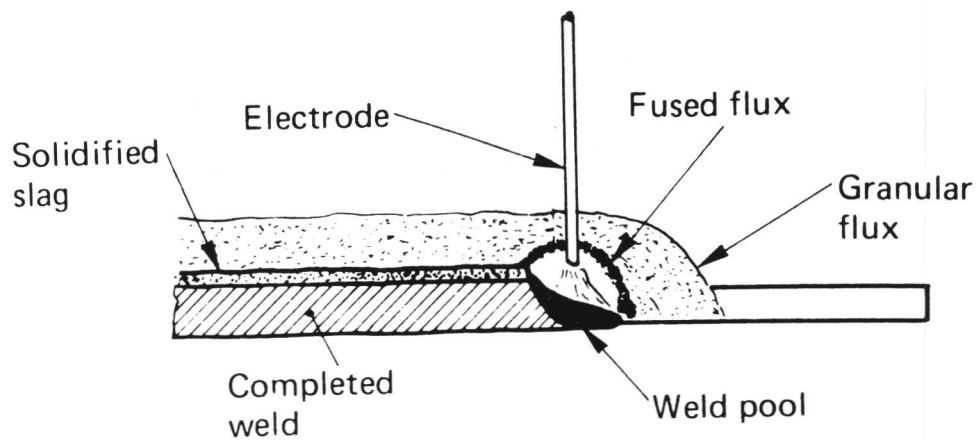


Figure 1.2: The SA welding process. (After L. M. Gourd (1980), "Principles of Welding Technology", Edward Arnold, London, U.K., 34).

butions.

Since the melt has approximately the same composition as the base metal, wetting of the base metal is very efficient, and the wetting angle,  $\theta \approx 0$ . This effectively reduces the energy required for nucleation to a point where there is almost no barrier to solidification, and it is only when inoculants are introduced into the weldpool that heterogeneous nucleation theory needs to be taken into account. The base metal acts as a very efficient heat sink, and solidification nuclei form at the oxide-free surface of the melted-back base material. Since heterogeneous nucleation is not expected in weldpools, the chill-cast layer characteristic of ingots cast in moulds is eliminated.

During solidification, certain grains at the base metal will be better oriented than others for  $\langle 100 \rangle$  growth with respect to the isotherms of the melt, and, in a way exactly analogous to the competitive growth found in ingot solidification, these quickly predominate and widen at the expense of others. The initial low rates of crystal growth are associated with a relatively planar solidification front. As the thermal gradient towards the centre of the pool decreases, the growth rate increases, and the morphology of the front changes through cellular to cellular-dendritic. Even independent nucleation of dendrites ahead of the solidification front may occur. It should be noted that dendritic and cellular substructures in welds tends to be on a finer scale than those in castings. This is mainly due to the comparatively high solidification rates of weld metal.

The cell spacing will affect the degree of solute segregation at the cell or dendritic boundaries with finer spacings giving less segregation. This segregation is a consequence of solute accumulation in grain-boundary grooves. The important factors in determining its magnitude are:

- (i) The density and spacing of the cell boundaries,
  - (ii) the partition coefficient of the solute,
- and (iii) the total amount of solute present (Easterling, 1983).

Most rapid weldpool solidification occurs at the centre of the bead, which would thus be expected to have the finest solidification substructure. The actual size of the cellular substructure is found to increase linearly relative to the reciprocal

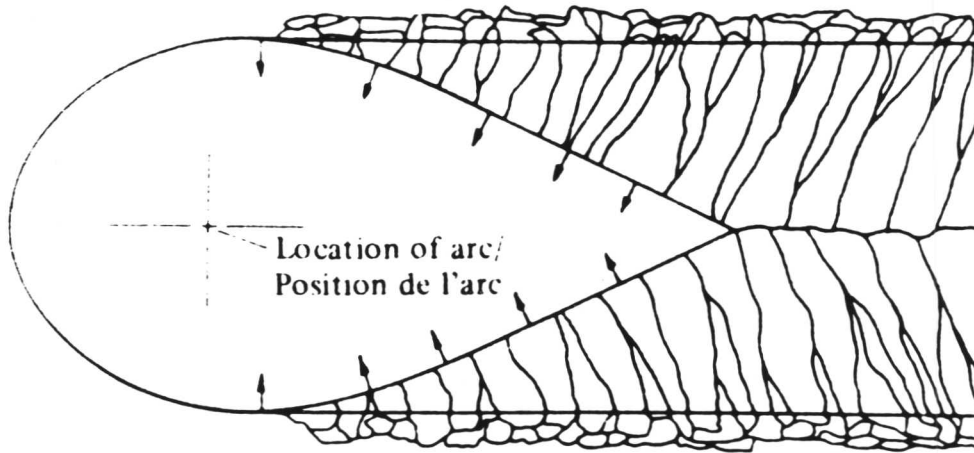
of the thermal gradient at the solid-liquid interface (Savage, 1980). The general coarseness of the microstructure at the fusion boundary is largely determined by the initial grain size of the base metal. Unfortunately, the base metal at the transition zone receives the most severe thermal cycle, and the grains in this zone tend to grow and become relatively coarse.

The speed of welding has an important influence on the eventual weld microstructure. During welding, growing crystals will try to follow the steepest temperature gradients. The maximum temperature gradient in a weldpool is normal to the pool boundary at all points of the boundary, and the distance between isotherms is inversely proportional to the welding speed. Thus, the form of the competitive growth process in a given material is uniquely controlled by the weldpool geometry.

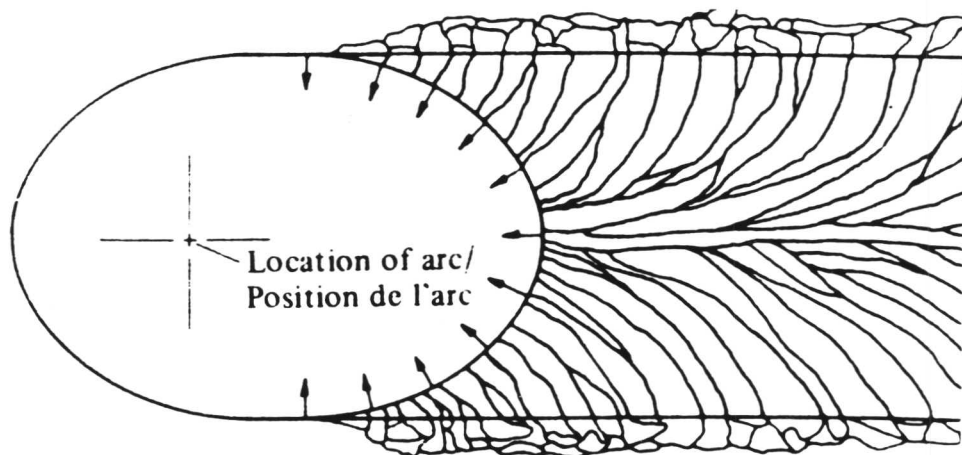
The effect of increasing the welding speed is to change the shape of the weld from an elliptical shape to a narrower tear shape. A tear-shaped weldpool, (Fig. 1.3a) maintains fairly constant thermal gradients up to the weld centreline because of the more angular geometry of the weld. On this basis, crystals are not required to change their growth directions as at slower speeds, and appropriately oriented crystals stabilise and widen, outgrowing crystals of less favourable orientation. With an elliptical weldpool, as shown in Figure 1.3b, the progressive change in the direction of the maximum thermal gradient is reflected in the survival of many more columnar grains. Since the maximum temperature gradients are constantly changing direction as the heat source moves away, the growing columnar crystals are faced with the necessity of trying to follow the maximum temperature gradients while still maintaining their preferred  $\langle 100 \rangle$  growth direction. Consequently, a columnar grain which survives over any great distance in a weldpool exhibits considerable curvature due to the progressive change in the favoured growth direction. The crystallographic orientation of the grain is maintained by repeated side-branching of the solidification substructure. If such growth becomes difficult for a number of adjacent grains due to the relative orientation of the easy growth direction and the continually changing direction of the maximum thermal gradient, a new columnar grain may be initiated from a random solid fragment incorporated into the interface from the melt. This fragment will have a  $\langle 100 \rangle$  direction oriented parallel to the direction of the maximum thermal gradient at the moment of solidification.

Once started, columnar growth normally dominates weldpool solidification.

a)



b)



Figures 1.3a and b: Schematic diagrams showing competitive growth with (a) a teardrop shaped weldpool, and (b) an elliptical weldpool. (After W. F. Savage (1980), *Weld. World*, 18, 93).

However, high welding speeds have been found to be particularly associated with a transition from predominantly columnar crystal growth to equiaxed growth at the final stage of solidification. This transition is thought to be due to the high amounts of segregation associated with the final stages of weldpool solidification. The shallow thermal gradient at this stage leads to high degrees of constitutional supercooling, and therefore the driving force for random dendritic growth to occur is large. This is compounded by the higher welding speeds which tend to cause overlap of the regions of solute accumulation ahead of the converging solidification front at the centre of the characteristically pear-shaped pool.

## 1.4 THE AS-DEPOSITED MICROSTRUCTURE

During the solidification of steel weld metals, solidification occurs either as  $\delta$ -ferrite followed by the formation of austenite, or as austenite directly. (This behaviour is discussed in Chapters 2 and 4). In the former case, the austenite grains will usually be on a finer scale than the  $\delta$ -ferrite columnar grains indicating that, on average, more than one nucleation event occurs at the  $\delta$ -ferrite grain boundary during the transformation (Widgery and Saunders, 1975). Growth is anisotropic along the grain boundaries and results in a columnar austenite grain structure resembling that of the original  $\delta$ -ferrite.

The final microstructure of the low-alloy steel weld evolves during the  $\gamma \rightarrow \alpha$  transformation when a variety of microstructural constituents may form, depending upon the chemical composition and cooling rate. However, the most important are allotriomorphic ferrite, Widmanstätten ferrite, and acicular ferrite. It should be noted that in the past, allotriomorphic ferrite has sometimes been referred to as proeutectoid ferrite or grain boundary ferrite, but these appellations do not differentiate between allotriomorphic ferrite and Widmanstätten ferrite, both of which can form above the eutectoid temperature, and at austenite grain boundaries.†

### 1.4.1 Allotriomorphic Ferrite

Allotriomorphic ferrite ( $\alpha$ ) usually forms between 1000 and 650°C during the cool-

---

† The very many terminologies which have been used to classify weld metal microstructures have been satisfactorily reviewed by the Japanese Welding Society (1983). The subject is not elaborated here, since such classifications are not based on transformation kinetics.

ing of steel weld deposits. Nucleation occurs heterogeneously at the austenite grain boundaries, often with one interface assuming a rational orientation relationship with the austenite. The adoption of a second one with the neighbouring grain resulting in faceted allotriomorphs on the grain boundary. Subsequent growth is extremely rapid, with the allotriomorphic ferrite forming an almost continuous layer of polycrystalline ferrite.

Allotriomorphic ferrite appears to grow in weld deposits without the redistribution of substitutional alloying elements during transformation (whose concentration will be low anyway). The growth rate is thus controlled by the diffusion of carbon into the remaining austenite (Bhadeshia *et al.*, 1985a). This mechanism of growth is termed *paraequilibrium* (Hillert, 1969), and occurs as a consequence of the fast cooling rates experienced by welds.

Allotriomorphic ferrite is perceived as being detrimental to the toughness of welds. This can be attributed to its relatively coarse grain size, and also its morphology, the continuous layers of which provide minimal resistance to crack propagation (Levine and Hill, 1977; Tweed, 1982).

#### 1.4.2 Widmanstätten Ferrite

Further cooling results in the formation of Widmanstätten ferrite ( $\alpha_w$ ). Primary Widmanstätten ferrite nucleates directly from those regions of the austenite grain boundaries not covered by allotriomorphic ferrite. Secondary Widmanstätten ferrite nucleates on the allotriomorphic ferrite grains at the  $\alpha/\gamma$  boundaries. The phase grows as sets of parallel plates separated by thin regions of austenite. Ultimately, the austenite remains in the weld as retained austenite, martensite and degenerate pearlite, known collectively as microphases (see below). The characteristic microstructure of Widmanstätten ferrite and microphases is referred to in welding institute nomenclature as “Ferrite with Aligned-Martensite-Carbide” (Figure 1.4).

Widmanstätten ferrite is the product of a displacive transformation, yet is able to form at low undercoolings below  $Ae_3$  by the cooperative growth of pairs of back-to-back plates whose shape changes largely cancel each other out (Bhadeshia, 1980). The characteristic wedge shape is a consequence of the slight misorientation of the habit planes of these two variants.

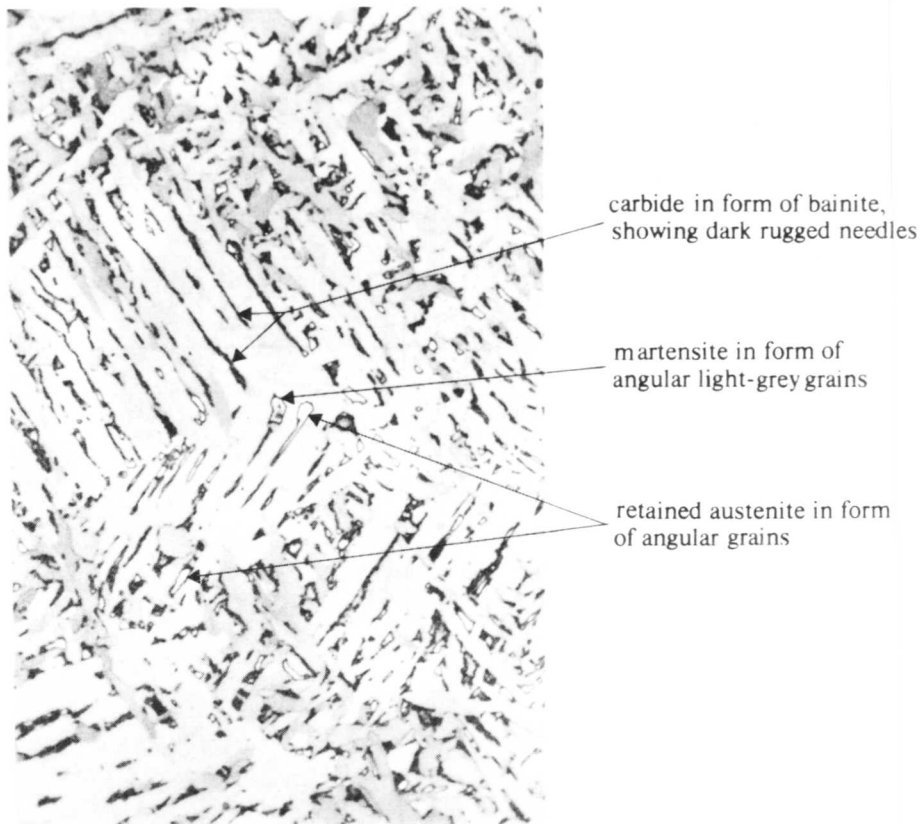


Figure 1.4: Widmanstätten ferrite with aligned M-A-C in submerged-arc weld metal. ( $\times 1000$ , reduced by one-third in reproduction). (After Almquist *et al.* (1972); cited in "Metallurgy of Welding", J. F. Lancaster (1987), 4<sup>th</sup> Ed., Allen & Unwin (Publishers) Ltd., London, U.K., 165).

Widmanstätten ferrite is perceived to be an undesirable constituent in weld deposits because of its inferior toughness properties (Devletian and Wood, 1983; Taylor and Farrar, 1975).

### 1.4.3 Acicular Ferrite

Acicular ferrite ( $\alpha_a$ ) is peculiar to steel weld metals, and forms within the columnar austenite grains in competition with Widmanstätten ferrite. Optically, it appears as a fine-grained interlocking array of non-parallel laths, as shown in Figure 1.5.

Until recently, the identity of the acicular ferrite phase had not been established. Recent work (Strangwood and Bhadeshia, 1987; Yang and Bhadeshia, 1987), however, has shown that acicular ferrite is bainite. The acicular ferrite plates form by a diffusionless and displacive transformation immediately after which, carbon is partitioned into the residual austenite. The transformation does not then obey the lever rule, and exhibits an incomplete reaction phenomenon, wherein the reaction ceases well before the residual austenite achieves its equilibrium carbon concentration.† Acicular ferrite differs morphologically from classical sheaf-like bainite firstly because it nucleates intragranularly, either on inclusions, or sympathetically on pre-existing plates, and secondly because growth is limited by physical impingement with other plates which form on neighbouring sites.

Acicular ferrite is a highly desirable constituent in steel weld metals. The large number of non-parallel grain boundaries hinder crack propagation, and impart good toughness to the weld (Widgery, 1974; Garland and Kirkwood, 1975; Taylor and Farrar, 1975). However, as with the other constituents of the microstructure, quantitative information as to its individual contribution to weld metal strength and toughness would be desirable.

### 1.4.4 Microphases

A fourth category of microstructural constituent are microphases, which are the last constituents to form in the weld. Microphases correspond to the small carbon-rich regions in the weld where the last remaining volumes of austenite transform, and consist of mixtures of martensite, carbides, degenerate pearlite, bainite, and retained austenite. As well as being located between the parallel plates of Widmanstätten ferrite, they form among the non-parallel plates of acicular ferrite.

---

† This is discussed at length in Chapter 10.

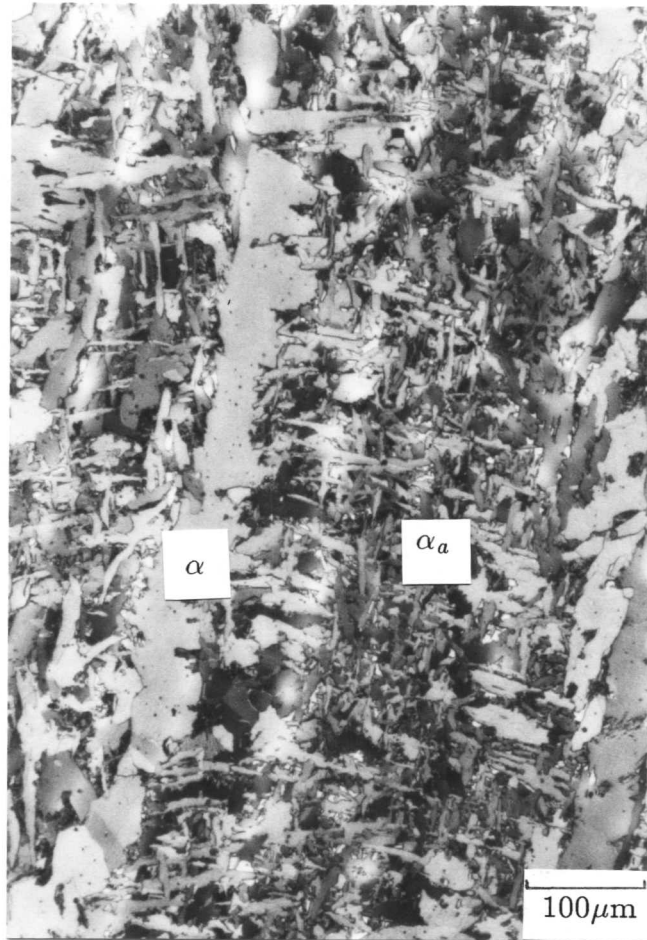


Figure 1.5: Acicular ferrite and allotriomorphic ferrite in a low-alloy steel weld deposit.

From the nature of the transformation products which comprise microphases, it is evident that a high volume fraction will have an adverse effect on weld metal properties.

#### 1.4.5 Idiomorphic Ferrite

Idiomorphic ferrite, which was first defined in the Dubé classification (1948) has a roughly equiaxed morphology and forms intragranularly. It is sometimes believed to form in steel welds when it is often classified as intragranular polygonal ferrite (Duncan, 1986). However, no evidence has been produced that it does not arise as a consequence of sectioning effects, and, in any case, the volume fraction in welds is always small and usually nil.

### 1.5 INCLUSIONS

Inclusions in weld metals primarily originate from oxides formed during weld deposition, or from the unintentional trapping of slag-forming materials which are used to protect the molten metal during welding. Non-metallic inclusions can be classified into three types. Primary indigenous inclusions are those deoxidation products which form if the saturation point of the inclusion-forming elements is exceeded during cooling, and have dimensions ranging from 1 to  $3\mu\text{m}$ . Secondary indigenous inclusions form as a consequence of the enrichment of the intercellular liquid that occurs during solidification. These particles are effectively trapped in the weld metal. They are characteristically much smaller than primary indigenous inclusions, having dimensions of the order of  $0.5\mu\text{m}$ , although unlike primary indigenous inclusions, their size is strongly dependent upon the cooling rate. The third type are exogenous inclusions. These are comparatively large non-metallic particles of external origin, up to  $10\mu\text{m}$  in diameter, which are picked up during the welding process, usually from the consumable or the slag, and become entrapped in the steel (Craig *et al.*, 1979). Exogenous inclusions are particularly undesirable, making for low weld metal toughness (Judson and McKeown, 1982). The mean inclusion diameter in low-alloy steel weld deposit can typically be about  $0.3\mu\text{m}$  (Dolby, 1983; Abson, 1978), although some inclusions as large as  $1\mu\text{m}$  (Steel, 1972) are sometimes found. The chemical compositions of inclusions are very complicated and depend on the particular welding process used.

It has often been suggested in the literature that a high inclusion volume frac-

tion should lead to a decrease in the austenite grain size of a weld deposit as a consequence of grain boundary pinning. Cochrane and Kirkwood (1979), Barritte *et al.* (1981), Harrison and Farrar (1981), and Ferrante and Farrar (1981) all reported experiments in which welds with different oxygen concentrations were reheated into the  $\gamma$  phase field and held there to allow coarsening. The resultant equiaxed grains were found to decrease in size with increasing oxygen content, and, since the volume fraction of inclusions in a weld correlates strongly with the total oxygen content, since most of the oxygen is present as oxides, and since most inclusions are oxides, the inference was that inclusions can restrict weld metal grain size. However, their experiments are not relevant to the as-welded microstructure, since they deal with *reheating* weld metal, when the austenite grain size is controlled by coarsening and driven by the  $\gamma/\gamma$  surface energy per unit volume, a driving force amounting to only a few J/mol. In contrast, the driving force for the formation of austenite from  $\delta$ -ferrite is relatively large compared to the force required to pin boundaries, and increases indefinitely with undercooling below the equilibrium transformation temperature. In such circumstances, pinning is not tenable (Yang, 1987).

Inclusions act as stress-concentrators in weld metals, and their rôle in weld metal fracture is well documented (Tweed and Knott, 1983; Knott, 1984; McRobie, 1985). Accordingly, it is desirable that their volume fraction should be kept to a minimum. However, further to this, it is now recognized that the size, type, and even size distribution of the inclusions is important (Cochrane and Kirkwood, 1979; Ferrante and Farrar, 1982; Cochrane, 1983). Although they are a prerequisite for the nucleation of acicular ferrite, above a low critical volume fraction they are unlikely to alter materially the volume fraction of acicular ferrite in a weld (Oldland, 1985). Thus, it is found that the model due to Bhadeshia *et al.* (1985a) discussed below can predict the volume fraction of acicular ferrite in a weld without a knowledge of the inclusion population.

## 1.6 A MODEL FOR THE AS-DEPOSITED MICROSTRUCTURE

In 1985, a model was proposed by Bhadeshia *et al.* (1985a; 1985b) by which the microstructure of the fusion zone of a weld metal might be estimated as a function of a few key welding variables. Subsequent work (Svensson *et al.*, 1986, Gretoft *et al.*, 1986, Bhadeshia *et al.*, 1987) has been shown this model to be extremely

successful, and it is now possible to predict quantitatively the volume fractions of the phases present in the as-deposited region of an MMA weld for a given chemical composition and set of welding variables. An outline of the model is given below.

The model assumes the prior austenite grains to have the morphology of space-filling hexagonal prisms, and Figure 1.6 shows one such grain in cross-section. The first stage during the decomposition of austenite is the formation of a uniform layer of allotriomorphic ferrite at the austenite grain boundaries. This is followed by the growth of Widmanstätten ferrite from the austenite boundaries as depicted in the second hexagon. Then, depending upon the growth rate of the Widmanstätten ferrite, it either impinges with the allotriomorphic ferrite on the other side of the grain, or with acicular ferrite nucleated on inclusions (depicted as black dots in Figure 1.6) within the grains.

Figure 1.7 illustrates the steps involved in the calculation of microstructure. With a knowledge of the chemical composition of the weld, and an estimation of the amount of solute segregation in the microstructure, thermodynamic theory allows phase diagrams and TTT curves to be calculated for solute-enriched and solute-depleted regions of the microstructure using a computer program developed by Bhadeshia (1982). The calculations are valid for up to 5wt% total alloying element additions of C, Mn, Ni, Cr, Mo and V, providing all alloying elements stay in solid solution.

From the TTT curve, a CCT curve is derived using an Additive Reaction Rule (Christian, 1975), which allows the martensite, bainite, Widmanstätten ferrite and allotriomorphic ferrite start temperatures, respectively  $M_s$ ,  $B_s$ ,  $W_s$  and  $T_h$ , and the allotriomorphic ferrite finish temperature,  $T_l$ , to be calculated. Knowing the allotriomorphic ferrite half-thickness,  $q$ , and the cooling rate of the weld over the temperature range  $800 \rightarrow 500^\circ\text{C}$ , the time taken for the weld to cool from  $T_h$  to  $T_l$ ,  $t_1$ , can be calculated (Svensson *et al.*, 1986), and the volume fraction of allotriomorphic ferrite,  $V_\alpha$ , is then estimated from the geometry of the grains, ignoring their ends since their length is very much longer than their widths.

Initially it was assumed that the nucleation of allotriomorphic ferrite was not a critical step, so that the formation of allotriomorphic ferrite essentially involves the diffusional thickening of layers of grain boundary allotriomorphic ferrite (Bhadeshia *et al.*, 1985b). However, in some relatively heavily alloyed welds, this is unjustified

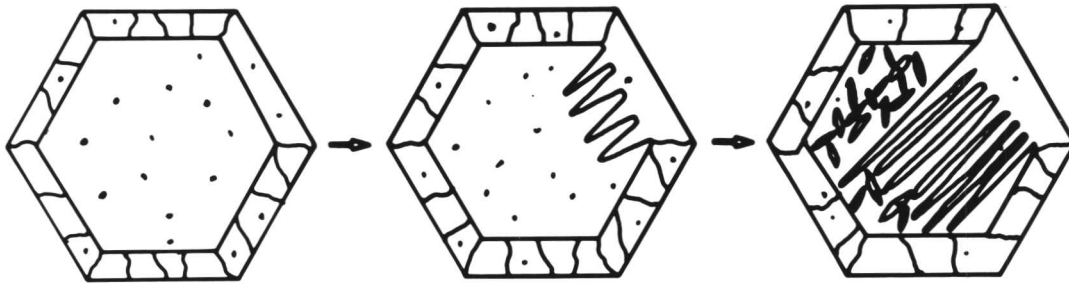


Figure 1.6: Schematic diagram showing the development of microstructure in a low-alloy steel weld deposit. (After H. K. D. H. Bhadeshia, L.-E. Svensson and B. Grefoet (1985), *Acta Metall.*, **33**, 1272).

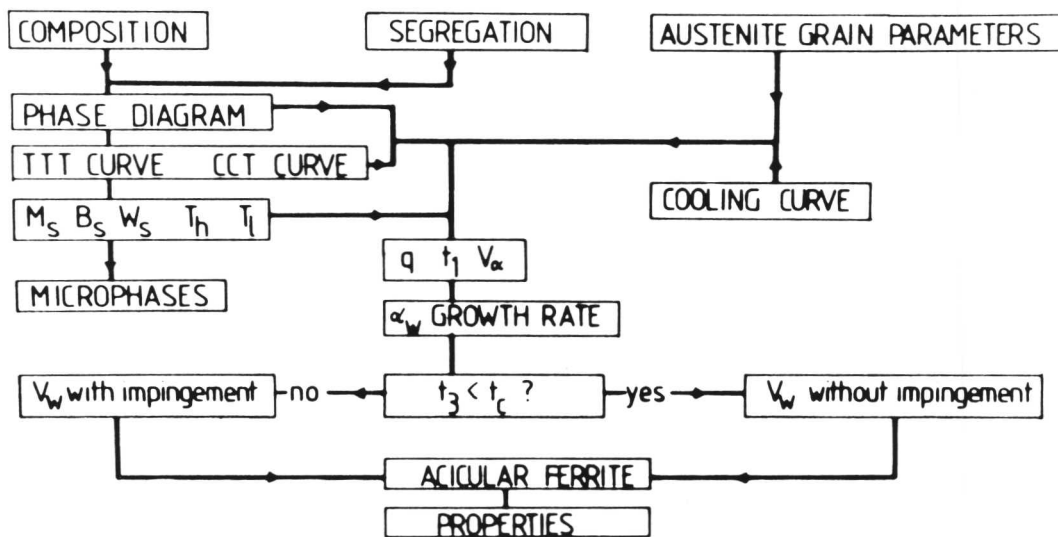


Figure 1.7: Flow diagram for the calculation of weld metal microstructure L.-E. Svensson and H. K. D. H. Bhadeshia (1988), "1988 International Conference of the International Institute for Welding", [*Proc. Conf.*], Pergamon Press, London, U.K., in press.

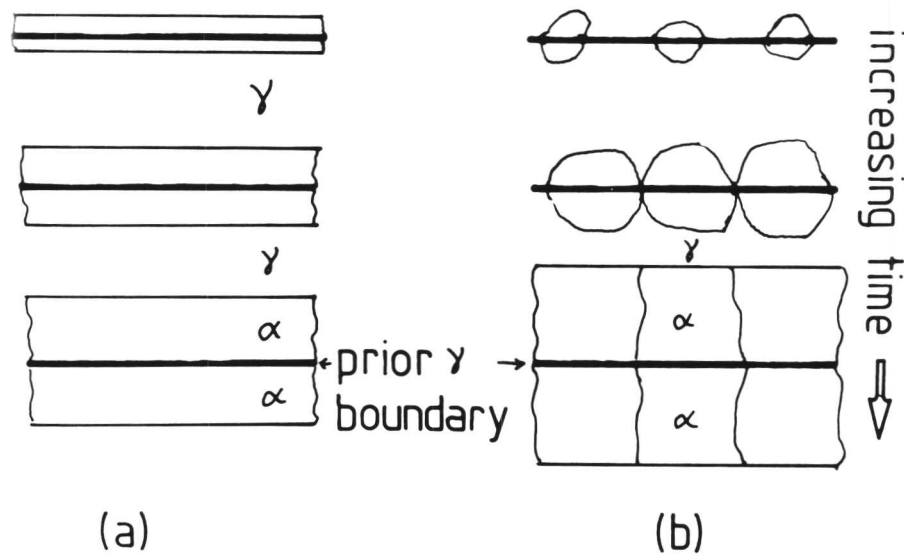


Figure 1.8: Diagram illustrating the growth of allotriomorphic ferrite as (a) the normal migration of the  $\alpha/\gamma$  interface, and (b) in the case of reality. (After H. K. D. H. Bhadeshia, L.-E. Svensson, and B. Grefott (1987), "Welding Metallurgy of Structural Steels", [*Proc. Conf.*], Met. Soc. A. I. M. E., Warrendale, Pa. 15086, 521).

since discontinuous layers of allotriomorphic ferrite are observed (Bhadeshia *et al.*, 1986). This is illustrated schematically in Figure 1.8. The model has since been refined to take account of allotriomorphic ferrite nucleation where site saturation does not occur at an early stage (Bhadeshia *et al.*, 1987).

Currently, the calculated volume fraction of allotriomorphic ferrite is approximately half that actually observed, and the theoretical volume fraction,  $V_\alpha$ , is modified from the calculated volume fraction,  $V_\alpha(\text{calc})$ , as

$$V_\alpha = 2.04\{V_\alpha(\text{calc})\} + 0.035 \quad (1.2)$$

However, this calculation for  $V_\alpha$  has been found to be very accurate at explaining the volume fraction of allotriomorphic ferrite in the primary microstructure with a correlation of 0.97 on the alloys analysed (Bhadeshia *et al.*, 1985a).

The volume fraction of microphases,  $V_m$ , can be estimated to a good approximation from the maximum volume fraction of martensite that can be observed from the untransformed austenite at the martensite start temperature, the latter being calculated assuming maximum growth of  $\alpha$ ,  $\alpha_w$ , and  $\alpha_a$ .

At  $t = t_l$ , the formation of Widmanstätten ferrite begins. The volume fraction is estimated by considering nucleation at the  $\gamma/\alpha$  interfaces, of which only a certain area fraction can nucleate. The  $\alpha_w$  grows sufficiently fast that growth may be treated as an isothermal process, based on a growth rate derived from Trivedi (Trivedi and Pound, 1969; Trivedi 1970a; 1970b).

By calculating whether  $\alpha_w$  grows with or without hard impingement with acicular ferrite within the austenite grains, *i.e.* if the time required for  $\alpha_w$  to grow across the austenite grains,  $t_3$ , is less than a critical time,  $t_c$ , the volume fraction of acicular ferrite can be estimated by

$$V_a = 1 - V_\alpha - V_w - V_m \quad (1.3)$$

Thus, the volume fraction of allotriomorphic ferrite, Widmanstätten ferrite, acicular ferrite and microphases in a weld can be estimated. Although, this model contains a number of approximations, it is fundamentally sound and predicts the

as-deposited microstructure with reasonable accuracy.

## 1.7 REAUSTENITISATION

In multirun weld deposits, the weld metal may be subject to not one but a series of thermal cycles of varying severity. Subsequent layers will reaustenitise part or all of those directly below them, with a consequent modification of structure. This additional transformation gives a characteristic microstructure consisting of approximately equiaxed grains, the coarseness of which increases with higher austenitisation temperatures, giving an increasing grain size up to the fusion boundary (Figure 1.9). Welding terminology is not clearly defined, and the reheated region may be referred to as the tertiary microstructure (Hoekstra *et al.*, 1986), or, as in this text, the secondary microstructure, depending upon whether one wishes to regard the as-welded microstructure as primary or derivative.

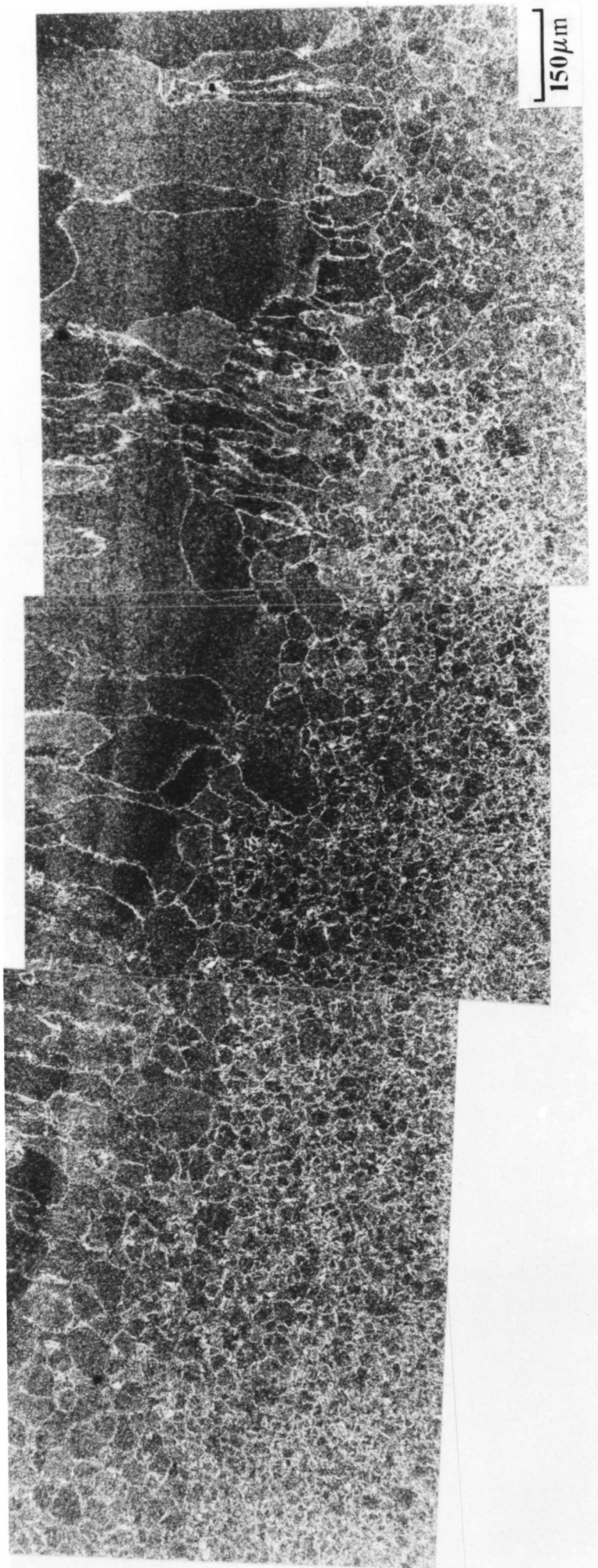
The secondary microstructure typically has a higher toughness and a lower strength than the as-welded microstructure, and research at Cambridge (Yang, 1987; Reed, 1988) is now particularly concerned with the construction of a model that will allow the prediction of the grain size, and explain the development of microstructure in this region. This is probably a prerequisite for the analytic prediction of the microstructure of multirun weld deposits.

The nucleation of austenite will be dependent upon the chemical composition and initial microstructure of the weld, and the severity of the weld thermal cycle. Its growth will depend upon the diffusion of carbon into the advancing interface. An exciting development has been the design of almost completely reheated high-strength multirun weld deposits, which exploit the good mechanical properties bestowed by reaustenitisation (Svensson and Bhadeshia, 1988). Careful alloy additions are used to produce a weld metal with an  $A_{e3}$  temperature sufficiently low that subsequent passes give a large volume of reheated material, and sufficient hardenability to give a tough, mechanically homogeneous, microstructure. The resultant weld exhibited an unusual combination of high strength and high toughness.

## 1.8 SUMMARY

This review has outlined the major factors that influence the development of micro-

Figure 1.9: Detail of a multirun weld deposit, illustrating the progressive refinement of weld metal grain size that occurs in the microstructure immediately beneath the weld run.



structure in the fusion zone of low-alloy steel weld deposits. Following transfer of the molten metal through the plasma of the arc, weld metal solidification is observed to occur at the parent metal interface. Although, the precise morphology of the solidifying interface is a function of the supercooling in the weldpool, grain growth is usually in the form of columnar grains, and this leads to an inhomogeneous distribution of alloying elements within the weld. At lower temperatures, decomposition of austenite in the weld gives rise to a characteristic microstructure consisting of grain boundary allotriomorphic ferrite, wedge-shaped parallel plates of Widmanstätten ferrite, and the fine-grained bainitic phase termed acicular ferrite. Microphases form later from the residual austenite.

While the essential theories of weld metal solidification are well understood, it is still not possible to analytically predict the solidification structure, and hence the distribution of solute in steel weld deposits. To enable this, research in this area should aim to provide quantitative data on the rates of cooling experienced in the initial stages of solidification, and, ideally, the problem should be approached both experimentally and thermodynamically, to allow a complete formal description to be developed.

Microstructurally, the model for the prediction of weld metal fusion zone has been successful, however, more work on the nature of the acicular ferrite phase is clearly desirable, since this phase is crucial for the design of high-strength high-toughness low-alloy C-Mn weldments. Also, the enormous importance of inclusions in influencing the microstructure and properties of low-alloy steel weld deposits has, until recently, been underestimated, and much systematic work should be addressed towards the understanding of their origin, and effects. An understanding of the factors that control their size and spatial distribution would be particularly welcome.

As regards the physical metallurgy of C-Mn weld deposits, there is much scope for work to relate mechanical properties, in particular tensile strength, toughness, and ductility, to the microstructure of both single-pass and multirun weld metals. These themes are all developed in the work that follows.

## REFERENCES

- ABSON, D. J. (1978), *Weld. Inst. Res. Rep.*, Welding Institute, Abington, U.K., 69/1978/M.
- BARRITTE, G. S., RICKS, R. A., and HOWELL, P. R. (1981), "Quantitative Microanalysis with High Spatial Resolution", Metals Society, London, U.K., 112-118.
- BHADESHIA, H. K. D. H. (1980), *Scripta Metall.*, **14**, 821-824.
- BHADESHIA, H. K. D. H. (1982), *Metal Sci.*, **16**, 159-165.
- BHADESHIA, H. K. D. H. (1985), *Prog. Mat. Sci.*, **29**, (4), 321-386.
- BHADESHIA, H. K. D. H., SVENSSON, L.-E., and GRETOFT, B. (1985a), *Acta Metall.*, **33**, 1271-1283.
- BHADESHIA, H. K. D. H., SVENSSON, L.-E., and GRETOFT, B. (1985b), *J. Mater. Sci. Lett.*, **4**, 305-308.
- BHADESHIA, H. K. D. H., SVENSSON, L.-E., and GRETOFT, B. (1986), "Welding and Performance of Pipe Welds", [*Proc. Conf.*], Welding Institute, Abington, U.K., paper 17.
- BHADESHIA, H. K. D. H., SVENSSON, L.-E., and GRETOFT, B. (1987), "Welding Metallurgy of Structural Steels", [*Proc. Conf.*], Met. Soc. A. I. M. E., Warrendale, Pa. 15086, 517-529.
- CHRISTIAN, J. W. (1975), "The Theory of Transformations in Metals and Alloys", 2nd Ed., Pergamon Press.
- COCHRANE, R. C. (1983), *Weld. World*, **21**, 16-24.
- COCHRANE, R. C. and KIRKWOOD, P. R. (1979), "Trends in Steels and Consumables for Welding", [*Proc. Conf.*], Welding Institute, Abington, U.K., 103-121.
- CRAIG, I, NORTH, T. H., BELL, H.B. (1979), *Ibid.*, 249-263.
- DAVIES, G. J. and GARLAND, J. G. (1975), *Int. Met. Rev.*, **20**, 83-106.
- DEVLETIAN, J. H. and WOOD, W. E. (1983), "Metals Handbook", 9<sup>th</sup> Edition, A. S. M., Metals Park, Ohio 44073, **6**, 21-49.
- DOLBY, R. E. (1983), *Met. Tech.*, **10**, 349-362.
- DUBE, C. A. (1948), Ph.D. thesis, Carnegie Institute of Technology.
- DUNCAN, A. (1986), *Weld. Inst. Res. Bull.*, Welding Institute, Abington, U.K.,

R318/8/86.

EASTERLING, K. E. (1983), "Introduction to the Physical Metallurgy of Welding", Butterworths, London, U.K.

FERRANTE, M., and FARRAR, R. A. (1981), *J. Mater. Sci.*, **17**, 3293-3298.

GARLAND, J. G. and KIRKWOOD, P.R. (1975), *Met. Constr.*, **7**, 275-283.

GOURD, L. M. (1980), "Principles of Welding Technology", Edward Arnold, London, U.K.

GRETOFT, B., BHADESHIA, H. K. D. H., and SVENSSON, L.-E. (1986), *Acta Stereol.*, **5**, (2), 365-371.

HARRISON, P. L. and FARRAR, R. A. (1981), *J. Mater. Sci.*, **16**, 2218.

HILLERT, M. (1969), "The Mechanism of Phase Transformations in Crystalline Solids", Institute of Metals, London, U.K., Monograph No. 13, 231.

HOEKSTRA, S., SCHMIDT-VAN DER BERG, M. A. M., and DEN OUDEN, G. (1986), *Met. Constr.*, **18**, (12), 771-775.

JAPANESE WELDING SOCIETY (1983), Committee of Welding Metallurgy, IIW-Doc. IX-1282-83.

JUDSON, P. and McKEOWN D. (1982), "2nd International Conference on Off-shore Welded Structures", [*Proc. Conf.*], Welding Institute, Abington, U.K., paper 3.

KNOTT, J. F. (1984), "Advances in Fracture Research", [*Proc. Conf.*], 6<sup>th</sup> International Conference on Fracture, Eds., S. R. Valluri, D. M. R. Taplin, P. Ramarao, J. F. Knott, and R. Dubey, Pergamon Press, Oxford, U.K.

LANCASTER, J. F. (1987), "Metallurgy of Welding", 4<sup>th</sup> Ed., Allen & Unwin (Publishers) Ltd., London, U.K.

LEVINE, E. and HILL, D. C. (1977), *Met. Constr.*, **9**, (8), 346-353.

LUNDQVIST, Berthold (1977), "Sandvik Welding Handbook", Sandvik AB, Sandvikken, Sweden.

McROBIE, D. E. (1985), Ph.D. thesis, University of Cambridge, U.K.

OLDLAND, R. B. (1985), *Aust. Weld. Res.*, (12), 31-43.

REED, R. C. (1988), Certificate of Postgraduate Study Dissertation, University of Cambridge, U.K.

- SAVAGE, W. F. (1980), *Weld. World*, **18**, 89-114.
- STEEL, A. C. (1972), *Weld. Res. Int.*, **2**, 37-76.
- STRANGWOOD, M. and BHADSHIA, H. K. D. H. (1987), "Advances in Welding Science and Technology", David, S. A., Ed., A. S. M., Metals Park, Ohio, 209-213.
- SVENSSON, L.-E. and BHADSHIA, H. K. D. H. (1988), "1988 International Conference of the International Institute for Welding", [*Proc. Conf.*], Pergamon Press, London, U.K., in press.
- SVENSSON, L.-E., GRETOFT, B., and BHADSHIA, H. K. D. H. (1986), *Scand J. Metall.*, **15**, 97-103.
- TAYLOR, L. G. and FARRAR, R. A. (1975), *Weld. Met. Fab.*, **43**, 305-316.
- TRIVEDI, R. (1970a), *Metall. Trans.*, **1**, 921-927.
- TRIVEDI, R. (1970b), *Acta Metall.*, **18**, 287-296.
- TRIVEDI, R. and POUND, G. M. (1967), *J. Appl. Phys.*, **38**, 3569-3576.
- TWEED, J. H. (1982), Ph.D. thesis, University of Cambridge, U.K.
- TWEED, J. H. and KNOTT, J. F. (1983), *Met. Sci*, **17**, 45-54.
- WIDGERY, D. J. (1974), Ph.D. thesis, University of Cambridge, U.K.
- WIDGERY, D. J. and SAUNDERS, G. G. (1975), *Weld. Inst. Res. Bull.*, **16**, 277-281.
- YANG, J.-R. (1987), Ph.D. thesis, University of Cambridge, U.K.
- YANG, J.-R. and BHADSHIA, H. K. D. H. (1987), "Advances in Welding Science and Technology", David, S. A., Ed., American Society for Metals, Metals Park, Ohio, 187-191.